

# Evaporation-Based Low-Cost Method for the Detection of Adulterant in Milk

Virkeshwar Kumar and Susmita Dash\*

Cite This: *ACS Omega* 2021, 6, 27200–27207

Read Online

ACCESS |



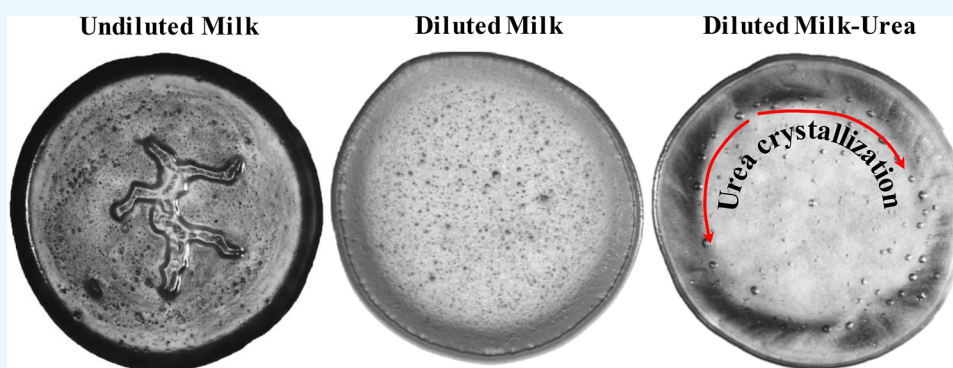
Metrics &amp; More



Article Recommendations



Supporting Information



**ABSTRACT:** Adulteration of milk poses a severe health hazard, and it is crucial to develop adulterant-detection techniques that are scalable and easy to use. Water and urea are two of the most common adulterants in commercial milk. Detection of these adulterants is both challenging and costly in urban and rural areas. Here we report on an evaporation-based low-cost technique for the detection of added water and urea in milk. The evaporative deposition is shown to be affected by the presence of adulterants in milk. We observe a specific pattern formation of nonvolatile milk solids deposited at the end of the evaporation of a droplet of unadulterated milk. These patterns alter with the addition of water and urea. The evaporative deposits are dependent on the concentrations of water and urea added. The sensitivity of detection of urea in milk improves with the dilution of milk with water. We show that our method can be used to detect a urea concentration as low as 0.4% in milk. Based on the detection level of urea, we present a regime map that shows the concentration of urea that can be detected at different extents of dilution of milk.

## 1. INTRODUCTION

Milk is a wholesome food source for mammals. It is enriched with calcium (important for bones) and other vital nutrients (carbohydrates, fats, protein minerals, and vitamins) required by both infants and adults.<sup>1–3</sup> Due to the increased public interest in high-protein diets, governmental support for milk consumption through school milk programs, and the vital dietary role of milk, developing countries usually encounter the issue of inadequate supply of milk for their large population.<sup>4,5</sup>

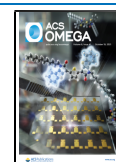
For monetary gains and maintaining the gap between demand and supply, vendors perpetrate the unethical practice of adulteration of milk. Milk adulteration is easy and very widespread, and poses severe health hazards.<sup>6</sup> For example, in 2018, 7% of the milk samples failed to match the standard milk quality decided by the Food Safety and Standards Authority of India.<sup>7</sup> In 2020, ~80% of open or packed milk sampled in some areas of Pakistan were reported to be adulterated with adulterants such as water, urea, soap, and formalin.<sup>8,9</sup> In 2020, it was reported that 2% of the milk samples were adulterated in China.<sup>10</sup> The adulterants can be classified into two types, namely (a) economically motivated adulterants, and (b) economically motivated and harmful adulterants.<sup>11</sup> Water,

vegetable protein, whey, and milk from different species (cow, buffalo, goat, sheep, camel, etc.) form the major constituents of economically motivated adulterants,<sup>11</sup> and these adulterants do not show severe health risk.<sup>11,12</sup> However, adulterants such as urea (to increase the nonprotein nitrogen content and whiteness consistency of milk), formalin and boric/benzoic acid (to increase the shelf life of milk), detergents (to emulsify the oil in diluted milk), chlorine (to compensate the density of the diluted milk after adulteration), and ammonium sulfate (to maintain the density of milk) pose severe health hazards.<sup>13,14</sup> These adulterants are harmful to the heart, liver, kidneys, and intestine and can even lead to death.<sup>14</sup> In the year 1850, 8000 infants lost their lives because of the Swill milk scandal in New York.<sup>11</sup> In 2008, the mixing of melamine (a chemical that is

Received: July 21, 2021

Accepted: September 28, 2021

Published: October 7, 2021



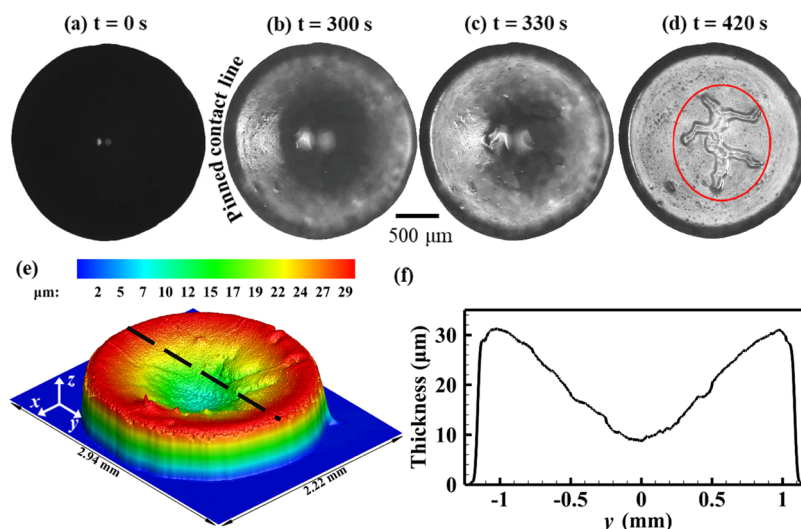


**Figure 1.** Top-view images of the evaporating unadulterated milk droplet with an initial volume =  $1 \mu\text{L}$  at different instants of time: (a)  $t = 0$  s, (b)  $t = 300$  s, (c)  $t = 330$  s (onset of amoeba-shaped pattern formation in the central region), (d)  $t = 420$  s, (e) variation of the thickness of the evaporation-induced deposit obtained using an optical profilometer, and (f) variation of thickness along the central line of deposit (dashed line marked in (e)).

used in fertilizers, concrete, and plastic) in milk powder caused the death of several infants in China.<sup>15</sup>

Water, primarily used to increase the volume of milk, is the most common adulterant, which alters the beneficial nutritive value, density, and foamy appearance of milk. Milk freezes at  $-0.55 \text{ }^\circ\text{C}$ , and the freezing point increases with the addition of water in milk.<sup>16</sup> Determination of freezing point is reported as one of the most sensitive methods and can detect water in excess of 3% added in milk.<sup>16</sup> Another popular method for the detection of added water in milk is based on the determination of solids-not-fat (SNF) content. The SNF (all of the nutrients excluding fat) decreases with the amount of water added; for example, SNF is  $\sim 9.1$  for undiluted milk and it is  $\sim 8.3$  for milk diluted with 10 wt % water.<sup>17</sup> In 2018, in India, 33.7% of the milk sampled possessed low SNF quality, and the average dilution was in the range of 2–20% of water.<sup>7,18</sup> The addition of water to milk is also detected by measuring the specific gravity of milk by a lactometer.<sup>19</sup> Milk adulterated with water is common in Asian countries (Bangladesh, China, India, Pakistan, etc.) compared to European countries, where the cost of milk is cheaper than water.<sup>18</sup> The water used in adulteration is often contaminated with the microorganisms and harmful chemicals (salt, urea, etc.), resulting in a serious health concern to the milk-consuming community.<sup>14</sup>

The addition of water to milk results in a reduction in whiteness and density, and to maintain these properties, urea is generally used as an adulterant.<sup>17,20</sup> Urea is one of the natural constituents of milk and accounts for 55% of the nonprotein nitrogen content of milk.<sup>17</sup> In milk, the quantity of urea can vary with cows and fodder and, in general, lies within 200–350 mg/L (0.02–0.035 wt %). The upper allowable limit of urea consumption is 0.07 wt % of milk. Urea is added as an adulterant to increase the shelf life and nonprotein nitrogen content, and maintain the SNF amount.<sup>21</sup> Urea is very cheap ( $\sim 0.07$  US cents/kg) and is commonly used to prepare synthetic milk. For instance, 55% of the milk sampled was detected with a high amount of urea in Brazil.<sup>18</sup> Urea is harmful to the kidney, liver, and other organs. The addition of urea to milk can be detected by using *para*-dimethyl amino benzaldehyde (DMAB).<sup>14,22</sup> In the standard procedure used by

the Food Safety and Standards Authority of India (FSSAI) and Food and Agriculture Organization (FAO), 1 mL of milk sample is mixed with 1 mL of 1.6% DMAB reagent (1.6 g of DMAB in 100 mL of ethyl alcohol and 10 mL of concentrated HCl), and a change in color is used as a test to determine the adulteration of milk by urea.<sup>22</sup> In another technique,<sup>11</sup> milk adulterated with urea, when added with urease and bromothymol, changes the color to bluish. In the above-discussed methods,  $\sim 0.2\%$  (wt/wt) urea is the limit of detection.

Biosensors for the detection of urea in milk have enabled a higher sensitivity of detection.<sup>23</sup> A robust and inexpensive manometric biosensor<sup>24,25</sup> used to detect urea in milk utilizes hydrolysis of urea with urease to release ammonium and carbonate ions, which in turn produce carbon dioxide, leading to a change in partial pressure. In a potentiometric biosensor,<sup>26</sup> urease hydrolyzes the urea, and ammonium ions are released. These ions create a potential difference across the transducer of the biosensor and aid in detection. In pH-based sensors, the urea in the milk undergoes a catalytic reaction with enzymes and releases ammonium ions, which change the pH value.<sup>27,28</sup> Although these sensors can handle a large number of samples in a short period and exhibit a detection limit of 0.0015% (wt/wt), the accuracy reduces with time.<sup>6,23</sup> For example, an enzyme-based urea biosensor loses its performance by 38% in 7 days.<sup>26</sup> Additionally, milk analyzers are expensive ( $\sim 400$  USD) and are difficult to incorporate in local agencies, where generally a smaller number of samples are processed. From the aforementioned aspects, it is clear that the detection of urea and water is still in the developing stage and is difficult to implement in rural areas.

The evaporation dynamics of a liquid mixture involving a nonvolatile solute, colloids, and a volatile solvent is a complex phenomenon due to the coupled effects of hydrodynamics, heat and mass transfer, and contact-line dynamics.<sup>20,29–33</sup> The evaporative deposition pattern is highly sensitive to the surface tension, surface tension gradient of the liquid, wettability and roughness of the underlying substrate, and nature of the solute.<sup>34–37</sup> While there have been several works on the evaporative deposition of colloidal particles on different

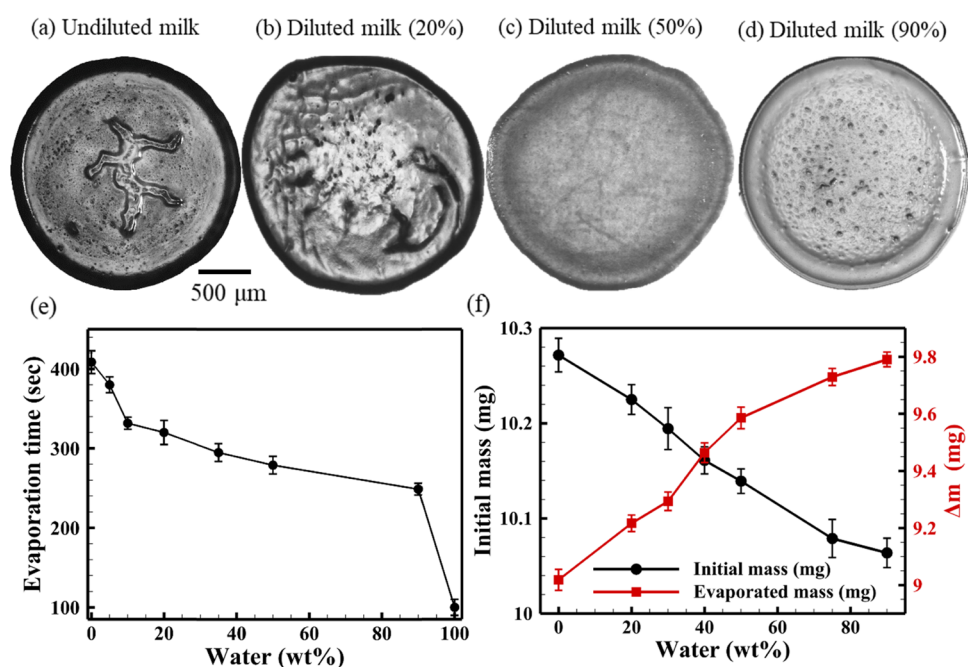


**Figure 2.** Final evaporative deposits for (a) undiluted milk showing the amoeba-shaped deposition pattern near the center; (b) diluted milk (20%) where the disintegration of structure in the final deposition occurs; (c) diluted milk (50%) with no distinct pattern formation in the droplet interior; and (d) diluted milk (90%). (e) Total evaporation time of milk at different extents of dilution, and (f) initial and evaporated mass ( $\Delta m$ ) of the diluted milk.

wettability substrates, the effect of dissolved solute on the deposition pattern is rather limited.<sup>34,38,39</sup> In aqueous saline drops, the salt crystallizes when the concentration exceeds the saturation concentration during evaporation.<sup>40,41</sup> The evaporative deposition is further affected by the presence of multiple components (evaporation of fuel,<sup>42</sup> ouzo droplets,<sup>43</sup> and surfactant in a binary mixture<sup>44</sup>). Recently, the differences in drying patterns of sessile droplets of blood have been reported as a means to detect diseases.<sup>45,46</sup> Milk is a complex fluid that contains nonvolatile milk solids (fats, protein, salt) and volatile (water-enriched material, ketones, alcohols, hydrocarbons, esters, etc.<sup>47</sup>) medium. Recently, evaporation of a pendant drop of milk was reported as a method to determine the percentage of milk solids.<sup>48,49</sup> The presence of added water and urea is expected to alter the deposition patterns formed after the evaporation of milk.

Here, we report on a plausible low-cost method to detect added urea (nonvolatile component) and water (volatile component) in milk using a simple evaporation-based method. In the case of milk adulterated with water, the final evaporative deposits show a reduction in the nonvolatile deposits along with a marked difference in the evaporative deposition pattern. During evaporation of milk adulterated with urea, evaporative mass loss results in the concentration of urea reaching a saturated concentration, which leads to the crystallization of urea. The distinct deposition pattern can be detected using a microscope or even a cell phone camera. We observe that evaporation-induced pattern formation can be used to detect an excess of 20 wt % added water and 8 wt % added urea in undiluted milk. The detection level of urea in milk improves drastically with the extent of dilution. In a 90% dilute solution of milk, the detection limit reaches as low as 0.4% urea. We present a regime map to show the detection limit of urea at different dilution levels of milk.

## 2. RESULTS AND DISCUSSION

### 2.1. Detection of the Economically Motivated Adulterant: Water in Milk.

Figure 1 shows the top-view images of a droplet of unadulterated milk evaporating on a glass slide maintained at 40 °C. Evaporation occurs due to the concentration difference of the volatile component of milk (mostly water, ketones, alcohols, and hydrocarbons) on the surface of the droplet and the ambient. The initial contact angle is  $\sim 22^\circ$  and the contact angle of the droplet changes to account for the evaporative mass loss. Further, the contact line remains pinned, leading to maximum evaporation near the triple contact line of the droplet.<sup>50,51</sup> This leads to a capillary-driven flow of the nonvolatile milk solids towards the pinned contact line, resulting in a well-known “coffee-ring” effect (Figure 1b,c).<sup>52</sup> The thickness of the deposit is maximum near the contact line (Figure 1e,f). Eventually, towards the end of evaporation, the milk solids form an “amoeba-shaped” deposition pattern (bounded by the red circle in Figure 1d) in the central region of the deposit that has a relatively lower thickness. Figure 1e,f shows the variation of the thickness of the evaporative deposits along the central line of the deposit measured using an optical profilometer. The amoeba-shaped pattern at the center of the deposit (Figure 1d) is consistently observed across all experiments using unadulterated milk. A similar amoeba-shaped pattern at the center of the deposit is observed on a nonheated substrate as well (details in the Supporting Information). The substrate temperature is maintained at 40 °C in the experiments to expedite evaporation while keeping the influence of temperature-induced convective flows minimum. For instance, the total time of evaporation for a 1  $\mu\text{L}$  droplet reduces from 11 min at room temperature (25 °C) to 7 min at 40 °C. Additionally, a similar evaporative deposition pattern is observed when the initial volume of the droplet is changed to 3 and 5  $\mu\text{L}$  (discussed in the Supporting Information).

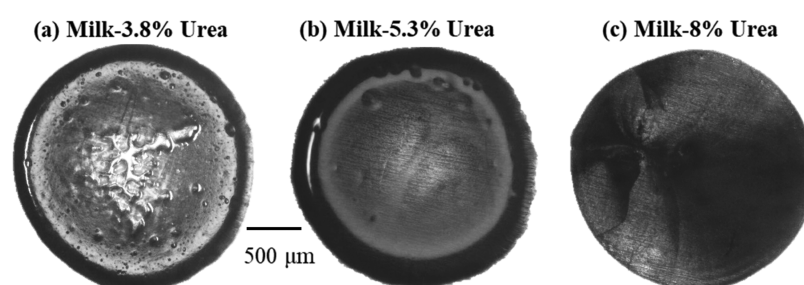


**Figure 3.** Final evaporative deposition of undiluted milk–urea mixture with (a) 3.8% urea, where a distinct amoeba-shaped pattern forms in the interior of the deposit, (b) 5.3% urea where the central deposition pattern is absent, and (c) 8% urea where crystallization of urea is observed towards the end of evaporation.

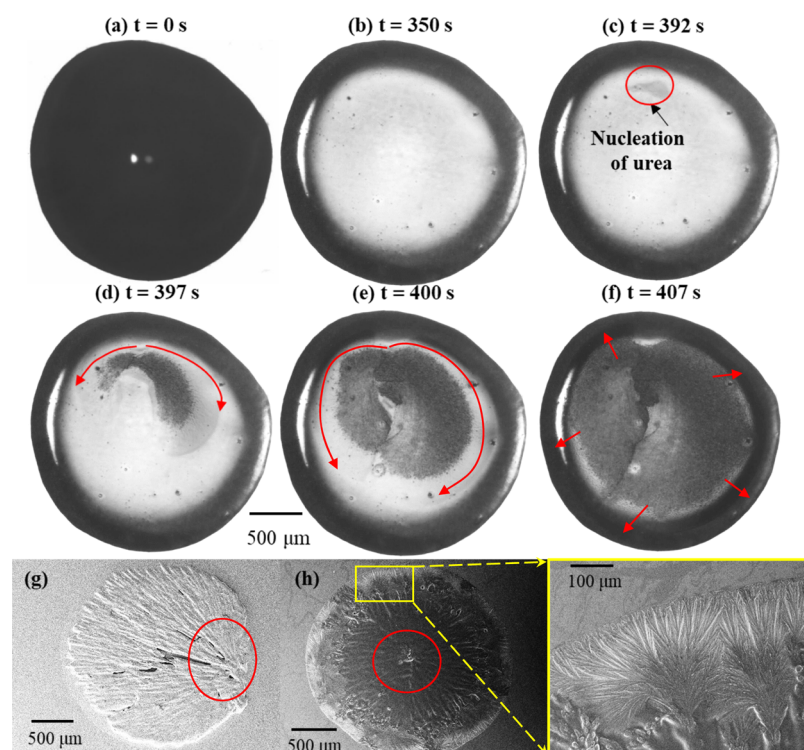


**Figure 4.** Top-view images of the evaporating droplet comprising 8% added urea in undiluted milk at (a)  $t = 0$  s, (b)  $t = 350$  s, (c)  $t = 392$  s; nucleation of urea crystal initiates in the interior of the droplet; (d, e)  $t = 397$ – $400$  s; the crystal grows along the periphery; (f)  $t = 407$  s (end of crystallization); the arrows represent the outward growth of crystal towards the pinned contact line. Scanning electron microscopy images of the crystallization pattern for cases where the nucleation of urea initiates (g) near the circumference of the droplet, and (h) near the central region of the droplet; the nucleation site is marked by a circle.

The elemental concentration at different spatial locations of the milk deposits, that is, at the pinned contact line, in the interior of the droplet, and at the center of the deposit (amoeba-shaped pattern), is determined using energy-dispersive X-ray spectroscopy (EDS). Except for the center of the deposit (amoeba-shaped pattern), all locations show a presence of calcium (2–5 wt %). The central deposit is primarily enriched with carbon (44.2 wt %) and oxygen (46 wt %), which suggests that these regions mainly comprise hydrocarbon/fats, which is different from the other regions. The details of the elemental analysis of the evaporative deposition are provided in the [Supporting Information](#).

The addition of water to unadulterated milk alters the final deposition pattern, especially in the interior of the deposit ([Figure 2a–d](#)). In diluted milk (20%), the distinct amoeba-shaped pattern disappears into spiral deposits towards the periphery of the deposit ([Figure 2b](#)). With a further increase in

the concentration of water in milk, these distinct patterns are absent in the final deposits ([Figure 2c,d](#)). The final deposition pattern formed at the end of evaporation is observed to be dependent on the amount of added water and can be distinguished even by the naked eye. Therefore, this method can be used as a physical means to detect the addition of water in milk.

The addition of water to milk increases the fraction of volatile content in the mixture, which leads to an increase in the rate of evaporation and reduction in the total evaporation time ([Figure 2e](#)). For instance, the total evaporation time of a 1  $\mu\text{L}$  droplet of unadulterated milk ( $\sim 400$  s) is significantly higher than that of deionized water ( $\sim 100$  s) ([Figure 2e](#)). The average evaporation rate is the lowest in undiluted milk (0.09 mg/s) and highest in diluted milk (90%) (0.16 mg/s) (the details are discussed in the [Supporting Information](#)).

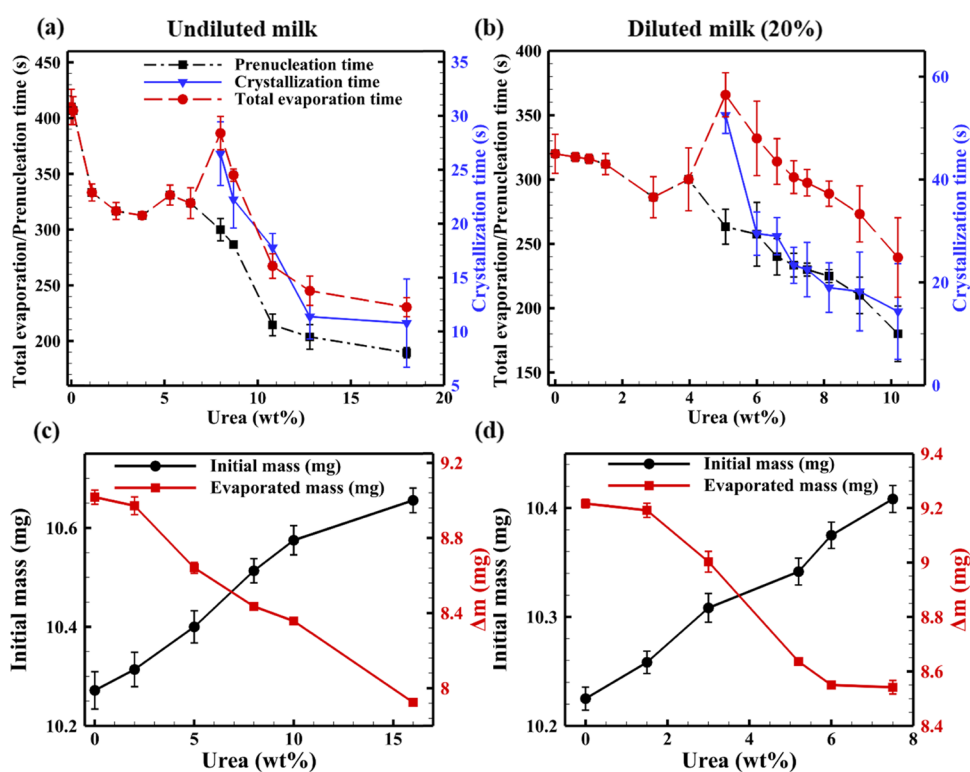


**Figure 5.** Variation of droplet evaporation time with varying initial urea concentration for the (a) undiluted milk–urea mixture and (b) diluted milk (20%)–urea mixture. Initial and evaporated mass for (c) undiluted milk–urea and (d) diluted milk (20%)–urea samples.

To determine the net evaporated mass, 10 drops (each with volume = 1  $\mu\text{L}$ ) are placed on a glass substrate, and the initial mass and the final mass after evaporation are measured by a weighing balance with an accuracy of 0.001 mg. The difference between the initial and final mass of 10 drops gives the evaporated mass ( $\Delta m$ ). For the same initial volume of the sample, unadulterated milk contains more nonvolatile components compared to the milk–water mixtures and therefore the evaporated mass is the lowest (Figure 2f).

As expected, the addition of water to milk results in a reduction in the average density (obtained from the measured mass and volume of droplets) of the milk–water mixture and can be used as another method to detect the presence of water (Figure 2f). For example, the density of milk changes from 1022  $\text{kg}/\text{m}^3$  with 20% dilution to 1016  $\text{kg}/\text{m}^3$  at 40% dilution with water. This reduction in density is due to the lower density of water (997  $\text{kg}/\text{m}^3$ ) compared to milk (1025–1030  $\text{kg}/\text{m}^3$ ). To summarize, the difference in the pattern of evaporative deposition, the difference in the density of the milk–water mixture, and evaporation dynamics can be used for the detection of added water in milk.

## 2.2. Detection of Harmful Adulterants: Urea in Milk.

Figure 3 shows the effect of added urea in undiluted milk on the final evaporation pattern. In the presence of a low weight percentage of urea (0–5%), the evaporative deposition pattern is observed to be similar to that of unadulterated milk (Figures 2a and 3a). As the percentage of added urea in undiluted milk is increased (5–8% urea), the distinct central deposition pattern disappears, and this regime can be identified as the “transition concentration” (Figure 3b). In these cases, the deposits are formed at the pinned contact line, whereas the amoeba-shaped pattern at the interior of the final deposit is absent. With a further increase in the concentration of urea

(>8% urea), we observe the crystallization of urea towards the end of evaporation (Figure 3c).

The temporal evaporation behavior of a droplet of undiluted milk adulterated with 8% urea is shown in Figure 4. Till 350 s (86% of the total evaporation time) (Figure 4b), the volatile component of milk evaporates and there is no internal pattern formation, similar to the case of transition concentration (Figure 3b). At  $t = 392$  s (96% of the total evaporation time), the concentration of urea reaches a saturation concentration ( $\sim 42$  to 46.5% of urea) and nucleation initiates suddenly in the interior of the droplet (marked by a circle in Figure 4c). The crystal grows on the substrate along the periphery of the outer deposit (the curved arrow shows the direction of growth of the crystallization of urea, Figure 4c–e) and subsequently towards the pinned contact line (Figure 4f). The directional growth of the crystals is also evident from the scanning electron microscopy images (Figure 4g,h); Figure 4g shows the nucleation site (marked by a circle) and directional growth of long crystals of urea in the droplet.

Further, we determine the detection limit of urea at different extents of dilution of milk. In the present work, milk is diluted with 20, 50, and 90% water. Further, these diluted samples are used to prepare milk–water–urea samples with different urea concentrations. The concentration of urea is varied till it is  $\sim 2$  times the detection concentration at different extents of dilution of milk. It is noted that crystallization of urea in the water–urea solution initiates near the triple contact line and proceeds along the periphery of the droplet.<sup>40</sup> However, we observe that in milk–urea or milk–water–urea mixtures, crystallization can also initiate at a location near the center of the droplet and not necessarily near the circumference of the droplet (Figure 4h). This may occur due to the localized variation of the concentration of urea in the presence of other

nonvolatile components of milk. Also, we hypothesize that the milk solids deposited in the interior of the droplet act as a nucleation site for the crystallization of urea. However, after nucleation, the crystal growth pattern is the same in all cases, and the crystal grows along the periphery of the droplet from the nucleation point. Towards the end of evaporation, the crystals grow outwards, towards the pinned contact line (Figure 4f). The evaporative crystallization of 0.6% urea in the diluted milk (90%)–urea mixture is discussed in the Supporting Information.

The duration of evaporation before the onset of nucleation of the urea crystal is termed as the prenucleation stage. The duration between the onset of nucleation and the end of crystallization is termed the crystallization stage. The total evaporation time is the sum of these two time periods (Figure 4a–f). In the case of milk–urea/milk–water–urea mixtures where urea does not crystallize distinctly (for example, undiluted milk with 3–5% urea, Figure 3a,b), the total evaporation time is the same as the prenucleation time. When the concentration of urea is increased, for instance, to 8% or more in undiluted milk, crystallization of urea is observed, and the total evaporation time is the sum of the prenucleation and crystallization times. The evaporation time decreases with the addition of urea (Figure 5). Interestingly, at initial urea concentrations greater than the transition concentration, the total evaporation time increases drastically. For instance, for undiluted milk with 8% urea the total evaporation time is 385 s, which is 20% longer than that of undiluted milk with 6.5% urea (Figure 5a). This increase in the evaporation time can be attributed to the longer duration of crystallization corresponding to critical initial concentrations where nucleation is observed (for instance, at 8% urea in the case of undiluted milk). With a further increase in the initial concentration of urea (greater than 8%), the crystallization time decreases because of the higher rate of crystallization for higher supersaturation of the solute.<sup>53</sup> For example, in undiluted milk with 11% urea, the crystallization duration is  $\sim 17 \pm 2.5$  s, whereas 8% urea crystallizes in  $\sim 26 \pm 4.8$  s (Figure 5a). Even for milk–water–urea mixtures, a similar behavior in terms of the total evaporation time is observed (Figure 5b).

The addition of urea increases the density of adulterated milk, as opposed to the addition of water that reduces its density. Therefore, a combination of water and urea is often used to maintain the density of adulterated milk. For example, while diluted milk (20%) has a density of  $1022 \text{ kg/m}^3$ , the addition of 3% urea in the diluted milk (20%) brings the density close to that of unadulterated milk ( $1030 \text{ kg/m}^3$ ). For a given extent of dilution, the density of the milk–water–urea mixture increases with an increase in the concentration of urea (Figure 5c,d). For instance, at 20% dilution, the density of the milk changes from  $1030 \text{ kg/m}^3$  at 3% urea to  $1034 \text{ kg/m}^3$  at 5% urea. The evaporated mass decreases with urea concentration, which indicates an increase in the nonvolatile content of the sample with urea. Additional data on the evaporation time and evaporation mass ( $\Delta m$ ) for diluted milk (50%) and diluted milk (90%) with added urea is provided in the Supporting Information.

### 3. GENERALIZED UREA DETECTION REGIME

The detection efficacy of urea in milk is observed to increase with the dilution of milk. We perform experiments at different extents of dilution and determine the critical concentration of urea that can be detected using the simple evaporation-based

method. For instance, the detectable threshold concentration of urea in undiluted milk is 8%. The presence of urea at a concentration as low as 0.4% is detectable in diluted milk (90%). Figure 6 shows a regime map depicting the detectable

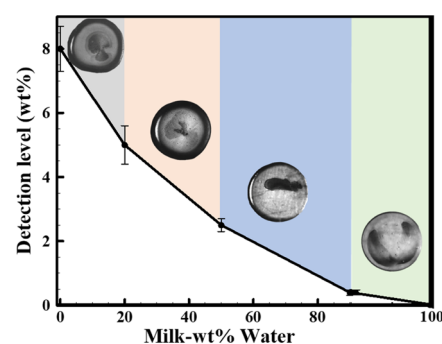


**Figure 6.** Regime map showing the detection level of urea in a milk–water–urea mixture. The insets represent images of evaporative crystallization at the corresponding ranges of dilution.

concentration of urea in the milk–water–urea mixture. The inset images in Figure 6 are representative of the evaporative crystallization of urea at different ranges of dilution. At a very high dilution of milk (90% water), the milk behaves nearly like pure water, and crystallization of urea is evident even at a very low concentration of urea. It should be noted that in a solution of deionized (DI) water–urea, the crystallization of urea is observed at a concentration above 0.02%. In view of this, if a diluted milk (20%) sample has an initial added urea concentration of 4%, which lies in the nondetectable range (Figure 6), the detection of urea can be made if we further dilute this sample to 90% (dilute milk (90%)–urea mixture). In this new diluted milk (90%), the corresponding urea concentration is 0.5%, which lies in the detection limit of the dilute milk (90%)–urea mixture (Figure 6). Thus, the method of dilution helps to detect low concentrations of added urea in milk. This evaporation-based method is a low-cost technique that requires a heated glass slide and a smartphone with a good zooming capacity to enable the detection of added urea in milk at any location.

### 4. CONCLUSIONS

In conclusion, we propose a simple evaporative deposition-based technique to detect the presence of two of the most common adulterants (water and urea) in milk. During evaporation, nonvolatile milk solids, as well as urea, exhibit an evaporative deposition and crystallization pattern that varies with the concentration of added water and urea in milk and can be used for the detection of adulterants in milk. We show that the density and rate of evaporation of adulterated milk vary with the concentration of water and urea. We develop a regime map that shows the detectable concentration of urea at different extents of dilution of milk. Using the proposed evaporative deposition-based technique, added water in excess of 20% and added urea as low as 0.4% can be detected. To summarize, while milk is a complex fluid and adulteration may not be restricted to only water or urea, this evaporation-based method opens up an avenue to explore the dependence of deposition pattern on the composition of milk and use it as a low-cost physical detection tool for detecting adulterants at home or any remote location.

## 5. EXPERIMENTAL SETUP

In the experiments, unadulterated commercial milk (with 3% fat and 8.5% SNF; certified by the International Organization for Standardization 22000) is used (the details are included in the [Supporting Information](#)). Deionized water and urea (Merck Emparta, >99.9% pure) are used for sample preparation. The experiments are performed using milk diluted with (0–90 wt/wt %) water. The dilution of milk is specified as the weight percentage of water added to milk. For example, diluted milk (20%) represents 20% wt/wt of water in milk. In these dilute mixtures, urea is added at different weight percentages and all the samples are represented as wt/wt%.

For evaporation experiments, a 1 mm thick glass slide is used as the test substrate. The substrate is cleaned by ultrasonication sequentially for 5 min each with DI water, acetone, and isopropyl alcohol (Merck Emparta, >99.9% pure). The cleaned glass slide is placed on a preheated hot plate (ThermoFisher Scientific) and maintained at 40 °C. The substrate temperature is measured using a K-type thermocouple and a handheld digital thermometer (Omega). During the experiments, the room temperature and relative humidity are maintained at 25 °C and 50%, respectively. A droplet of volume 1  $\mu\text{L}$  is deposited on the heated substrate using a precalibrated micropipette. The evaporation of the droplet is imaged from the top using a camera fitted to a microscope (Leica M205 A) to visualize the evolution of evaporation-induced pattern formation. The contact angle of pure milk on the glass slide is measured to be  $22 \pm 2^\circ$ . The contact angle reduces with the addition of water; for instance, for diluted milk (90%), the contact angle is measured to be  $16 \pm 1.8^\circ$ . The final evaporative deposition pattern is compared and correlated with the concentration of the adulterant. Each experiment is repeated at least 5 times and the observations are found to be repeatable. It should be noted that the evaporative patterns are observed to be similar even without the rigorous cleaning protocol.

## ■ ASSOCIATED CONTENT

### SI Supporting Information

The Supporting Information is available free of charge at <https://pubs.acs.org/doi/10.1021/acsomega.1c03887>.

Details of evaporation of undiluted milk from different sources; evaporation pattern of undiluted milk at different substrate temperatures and initial volume of the droplet; evaporation rate of the diluted milk droplet; elemental analysis by EDS; urea crystallization in a diluted milk–urea sample ([PDF](#))

## ■ AUTHOR INFORMATION

### Corresponding Author

Susmita Dash – Department of Mechanical Engineering, Indian Institute of Science Bangalore, Bengaluru 560012, India; [orcid.org/0000-0003-0952-4209](https://orcid.org/0000-0003-0952-4209); Phone: +91-080 2293 2962; Email: [susmitadash@iisc.ac.in](mailto:susmitadash@iisc.ac.in)

### Author

Virkeshwar Kumar – Department of Mechanical Engineering, Indian Institute of Science Bangalore, Bengaluru 560012, India; [orcid.org/0000-0001-6324-5679](https://orcid.org/0000-0001-6324-5679)

Complete contact information is available at:

<https://pubs.acs.org/doi/10.1021/acsomega.1c03887>

## Notes

The authors declare no competing financial interest.

## ■ ACKNOWLEDGMENTS

V.K. gratefully acknowledges the financial support from the C V Raman Postdoctoral Research grant, Indian Institute of Science Bangalore. S.D. acknowledges the Young Investigator grant received from Infosys Foundation. The authors also thank the SEM facility at the Advanced Facility for Microscopy and Microanalysis (AFMM) and the optical profilometer facility at the Centre for Nano Science and Engineering (CeNSE) at IISc Bangalore.

## ■ REFERENCES

- (1) Poetschke, P. The Chlorine Content of Milk. *J. Ind. Eng. Chem.* **1912**, *4*, 38–40.
- (2) Shelver, W. L.; Lupton, S. J.; Shappell, N. W.; Smith, D. J.; Hakk, H. Distribution of Chemical Residues among Fat, Skim, Curd, Whey, and Protein Fractions in Fortified, Pasteurized Milk. *ACS Omega* **2018**, *3*, 8697–8708.
- (3) Wei, B.; McGuffey, J. E.; Blount, B. C.; Wang, L. Sensitive Quantification of Cannabinoids in Milk by Alkaline Saponification–Solid Phase Extraction Combined with Isotope Dilution UPLC–MS/MS. *ACS Omega* **2016**, *1*, 1307–1313.
- (4) Griffin, M. *Overview of Worldwide School Milk Programmes*, 3rd International School Milk Conference, FAO, Kunming, 2005; pp 1–10.
- (5) Di Giovanni, S.; Zambrini, V.; Varriale, A.; D’Auria, S. Sweet Sensor for the Detection of Aflatoxin M1 in Whole Milk. *ACS Omega* **2019**, *4*, 12803–12807.
- (6) Das, S.; Goswami, B.; Biswas, K. Milk Adulteration and Detection: A Review. *Sens. Lett.* **2016**, *14*, 4–18.
- (7) Food Safety and Standards Authority of India. *National Milk Safety & Quality Survey*; 2018 report, FSSAI, 2018.
- (8) Muntaha, S. T.; Iqbal, R.; Yasmin, I.; Tehseen, S.; Khaliq, A.; Chughtai, M. F. J.; Ahsan, S.; Khan, W. A.; Nadeem, M.; Hleba, L.; Rebezov, M.; Khayrullin, M.; Kuznetsova, E.; Kozlovskikh, L.; Shariati, M. A. Safety Assessment of Milk and Indigenous Milk Products from Different Areas of Faisalabad. *J. Microbiol., Biotechnol. Food Sci.* **2020**, *9*, 1197–1203.
- (9) Barham, G. S.; Khaskheli, M.; Soomro, A. H.; Nizamani, Z. A. Extent of Extraneous Water and Detection of Various Adulterants in Market Milk at Mirpurkhas, Pakistan. *J. Agric. Vet. Sci.* **2014**, *7*, 83–89.
- (10) Yang, Y.; Zhang, L.; Hetingta, K. A.; Erasmus, S. W.; Van Ruth, S. M. Prevalence of Milk Fraud in the Chinese Market and Its Relationship with Fraud Vulnerabilities in the Chain. *Foods* **2020**, *9*, No. 709.
- (11) Azad, T.; Ahmed, S. Common Milk Adulteration and Their Detection Techniques. *Int. J. Food Contam.* **2016**, *3*, No. 22.
- (12) Li, L.; Wang, J.; Li, M.; Yang, Y.; Wang, Z.; Miao, J.; Zhao, Z.; Yang, J. Detection of the Adulteration of Camel Milk Powder with Cow Milk by Ultra-High Performance Liquid Chromatography (UPLC). *Int. Dairy J.* **2021**, *121*, No. 105117.
- (13) Gahukar, R. Food Adulteration and Contamination in India: Occurrence, Implication and Safety Measures. *Int. J. Basic Appl. Sci.* **2013**, *3*, No. 1727.
- (14) Reddy, M.; Venkatesh, K.; Venkata, C.; Reddy, S. Adulteration of Milk and Its Detection: A Review. *Int. J. Chem. Stud.* **2017**, *5*, 613–617.
- (15) Qjana, G.; Guoa, X.; Guob, J.; Wub, J. China’s Dairy Crisis: Impacts, Causes and Policy Implications for a Sustainable Dairy Industry. *Int. J. Sustain. Dev. World Ecol.* **2011**, *18*, 434–441.
- (16) Shipe, W. F. The Freezing Point of Milk. A Review. *J. Dairy Sci.* **1959**, *42*, 1745–1762.
- (17) Singh, P.; Gandhi, N. Milk Preservatives and Adulterants: Processing, Regulatory and Safety Issues. *Food Rev. Int.* **2015**, *31*, 236–261.

- (18) Handford, C. E.; Campbell, K.; Elliott, C. T. Impacts of Milk Fraud on Food Safety and Nutrition with Special Emphasis on Developing Countries. *Compr. Rev. Food Sci. Food Saf.* **2016**, *15*, 130–142.
- (19) Lampert, L. M. Nomograph for Correction of Lactometer Readings and Calculation of Milk Solids. *Ind. Eng. Chem. - Anal. Ed.* **1940**, *12*, 527–528.
- (20) Patari, S.; Mahapatra, P. S. Liquid Wicking in a Paper Strip: An Experimental and Numerical Study. *ACS Omega* **2020**, *5*, 22931–22939.
- (21) Kavitha, P. Studies on the Levels of Urea in Milk. MSc Thesis, ICAR-National Dairy Research Institute, Karnal, 2000.
- (22) Food Safety and Standards Authority of India. *Manual of Methods of Analysis of Foods: Milk and Milk Products*; Lab Manual Report, 2015.
- (23) Renny, E. F.; Daniel, D. K.; Krastanov, A. I.; Zachariah, C. A.; Elizabeth, R. Enzyme Based Sensor for Detection of Urea in Milk. *Biotechnol. Biotechnol. Equip.* **2005**, *19*, 198–201.
- (24) Sharma, R.; Rajput, Y. S.; Kaur, S.; Tomar, S. K. A Method for Estimation of Urea Using Ammonia Electrode and Its Applicability to Milk Samples. *J. Dairy Res.* **2008**, *75*, 466–470.
- (25) Jenkins, D. M.; Delwiche, M. J. Manometric Biosensor for On-Line Measurement of Milk Urea. *Biosens. Bioelectron.* **2002**, *17*, 557–563.
- (26) Trivedi, U. B.; Lakshminarayana, D.; Kothari, I. L.; Patel, N. G.; Kapse, H. N.; Makhija, K. K.; Patel, P. B.; Panchal, C. J. Potentiometric Biosensor for Urea Determination in Milk. *Sens. Actuators, B* **2009**, *140*, 260–266.
- (27) Brzózka, Z.; Dawgul, M.; Pijanowska, D. G.; Torbicz, W. Durable NH<sub>4</sub><sup>+</sup>-Sensitive CHEMFET. *Sens. Actuators, B* **1997**, *44*, 527–531.
- (28) Pijanowska, D. G.; Remiszewska, E.; Lysko, J. M.; Jaźwiński, J.; Torbicz, W. Immobilisation of Bioreceptors for Microreactors. *Sens. Actuators, B* **2003**, *91*, 152–157.
- (29) Dash, S.; Rapoport, L.; Varanasi, K. K. Crystallization-Induced Fouling during Boiling: Formation Mechanisms to Mitigation Approaches. *Langmuir* **2018**, *34*, 782–788.
- (30) McBride, S. A.; Skye, R.; Varanasi, K. K. Differences between Colloidal and Crystalline Evaporative Deposits. *Langmuir* **2020**, *36*, 11732–11741.
- (31) Cachile, M.; Bénichou, O.; Cazabat, A. M. Evaporating Droplets of Completely Wetting Liquids. *Langmuir* **2002**, *18*, 7985–7990.
- (32) Chung, D. C. K.; Huynh, S. H.; Katariya, M.; Chan, A. Y. C.; Wang, S.; Jiang, X.; Muradoglu, M.; Liew, O. W.; Ng, T. W. Drops on a Superhydrophobic Hole Hanging on under Evaporation. *ACS Omega* **2017**, *2*, 6211–6222.
- (33) Bozorgmehr, B.; Murray, B. T. Numerical Simulation of Evaporation of Ethanol-Water Mixture Droplets on Isothermal and Heated Substrates. *ACS Omega* **2021**, *6*, 12577–12590.
- (34) Park, J.; Moon, J. Control of Colloidal Particle Deposit Patterns within Picoliter Droplets Ejected by Ink-Jet Printing. *Langmuir* **2006**, *22*, 3506–3513.
- (35) McBride, S. A.; Dash, S.; Khan, S.; Varanasi, K. K. Evaporative Crystallization of Spirals. *Langmuir* **2019**, *35*, 10484–10490.
- (36) Shahidzadeh, N.; Schut, M. F. L.; Desarnaud, J.; Prat, M.; Bonn, D. Salt Stains from Evaporating Droplets. *Sci. Rep.* **2015**, *5*, No. 10335.
- (37) Deegan, R. D.; Bakajin, O.; Dupont, T. F.; Huber, G.; Nagel, S. R.; Witten, T. A. Contact Line Deposits in an Evaporating Drop. *Phys. Rev. E* **2000**, *62*, 756–765.
- (38) Dutta Choudhury, M.; Dutta, T.; Tarafdar, S. Growth Kinetics of NaCl Crystals in a Drying Drop of Gelatin: Transition from Faceted to Dendritic Growth. *Soft Matter* **2015**, *11*, 6938–6947.
- (39) Thampi, S. P.; Basavaraj, M. G. Beyond Coffee Rings: Drying Drops of Colloidal Dispersions on Inclined Substrates. *ACS Omega* **2020**, *5*, 11262–11270.
- (40) Schmid, J.; Zarihos, I.; Terzis, A.; Roth, N.; Weigand, B. Crystallization of Urea from an Evaporative Aqueous Solution Sessile Droplet at Sub-Boiling Temperatures and Surfaces with Different Wettability. *Exp. Therm. Fluid Sci.* **2018**, *91*, 80–88.
- (41) Wu, S.; Wu, D.; Huang, Y. Evaluation of the Crystallization Pressure of Sulfate Saline Soil Solution by Direct Observation of Crystallization Behavior. *ACS Omega* **2021**, *6*, 17680–17689.
- (42) Wilms, J. Evaporation of Multicomponent Droplets. PhD Thesis, 2005.
- (43) Tan, H.; Diddens, C.; Lv, P.; Kuerten, J. G. M.; Zhang, X.; Lohse, D. Evaporation-Triggered Microdroplet Nucleation and the Four Life Phases of an Evaporating Ouzo Drop. *Proc. Natl. Acad. Sci. U.S.A.* **2016**, *113*, 8642–8647.
- (44) Qazi, M. J.; Salim, H.; Doorman, C. A. W.; Jambon-Puillet, E.; Shahidzadeh, N. Salt Creeping as a Self-Amplifying Crystallization Process. *Sci. Adv.* **2019**, *5*, No. eaax1853.
- (45) Lanotte, L.; Laux, D.; Charlot, B.; Abkarian, M. Role of Red Cells and Plasma Composition on Blood Sessile Droplet Evaporation. *Phys. Rev. E* **2017**, *96*, No. 053114.
- (46) Kar, S.; Kar, A.; Chaudhury, K.; Maiti, T. K.; Chakraborty, S. Formation of Blood Droplets: Influence of the Plasma Proteins. *ACS Omega* **2018**, *3*, 10967–10973.
- (47) Toso, B.; Procida, G.; Stefanon, B. Determination of Volatile Compounds in Cows' Milk Using Headspace GC-MS. *J. Dairy Res.* **2002**, *69*, 569–577.
- (48) Harindran, A.; Hashmi, S.; Madhurima, V. Pattern Formation of Dried Droplets of Milk during Different Processes and Classifying Them Using Artificial Neural Networks. *J. Dispers. Sci. Technol.* **2021**, 1–10.
- (49) Lin, S. X. Q.; Chen, X. D. Changes in Milk Droplet Diameter during Drying under Constant Drying Conditions Investigated Using the Glass-Filament Method. *Food Bioprod. Process.* **2004**, *82*, 213–218.
- (50) Shahidzadeh-Bonn, N.; Rafai, S.; Bonn, D.; Wegdam, G. Salt Crystallization during Evaporation: Impact of Interfacial Properties. *Langmuir* **2008**, *24*, 8599–8605.
- (51) Jason, N. N.; Chaudhuri, R. G.; Paria, S. Self-Assembly of Colloidal Sulfur Particles Influenced by Sodium Oxalate Salt on Glass Surface from Evaporating Drops. *Soft Matter* **2012**, *8*, 3771–3780.
- (52) Mampallil, D.; Eral, H. B. A Review on Suppression and Utilization of the Coffee-Ring Effect. *Food Bioprod. Process.* **2018**, *252*, 38–54.
- (53) Naillon, A.; Joseph, P.; Prat, M. Ion Transport and Precipitation Kinetics as Key Aspects of Stress Generation on Pore Walls Induced by Salt Crystallization. *Phys. Rev. Lett.* **2018**, *120*, No. 034502.